Log Number: J22609 Final Version: Jan 3, 1997

Improved Damage Location Accuracy Using Strain Energy-Based Mode Selection Criteria*

Scott W. Doebling†

Los Alamos National Laboratory, Los Alamos, NM, 87545

Francois M. Hemez‡

Ecole Centrale Paris, Chatenay-Malabry 92295, France

Lee D. Peterson**, **Charbel Farhat**††

University of Colorado, Boulder, CO, 80309-0429

Abstract

A method is presented for selecting the subset of identified structural vibration modes to be used in finite element model correlation for structural damage detection. The method is based on a ranking of the modes using measured modal strain energy, and is a function of only the measured modal parameters. It is shown that a mode selection strategy based on maximum modal strain energy produces more accurate update results than a strategy based on minimum frequency. Strategies that use the strain energy stored by modes in both the undamaged and damaged structural configuration are considered. It is demonstrated that more accurate results are obtained when the modes are selected using the maximum strain energy stored in the damaged structural configuration. The mode selection techniques are

---

*Presented as Paper 93-1481 entitled "Selection of Experimental Modal Data Sets for Damage Detection via Model Update," at the 34th AIAA/ASME/ASCE/AHS/ASC Structures, Structural Dynamics, and Materials Conference, La Jolla, CA, April 1993.

†Technical Staff Member, Engineering Analysis Group (ESA-EA), Mail Stop P946, Los Alamos National Laboratory, Los Alamos, NM, 87545. Member AIAA.

‡Assistant Professor, Department of Mechanical Engineering of Soils, Structures, and Materials. Member AIAA

**Associate Professor, Center for Aerospace Structures and Department of Aerospace Engineering Sciences. Senior Member AIAA.

††Professor, Center for Aerospace Structures and Department of Aerospace Engineering Sciences. Senior Member AIAA.

applied to the results of a damage detection experiment on a suspended truss structure that has a large amount of localized modal behavior.

Nomenclature

Variables

A, $\hat{A}$	True and model-update values of cross-sectional area
K	Structural stiffness matrix
N_e	Total number of finite elements in model
U_j	Total strain energy stored in structure by mode j
Φ	Mode shape matrix
Λ	Diagonal matrix of modal frequencies squared

Superscripts

u	Undamaged state of structure
d	Damaged state of structure
e	Elemental property

Introduction

In the maintenance of aerospace and civil structures, the ability to evaluate the integrity of the structure is becoming an important technology. Inspection techniques that require physically dismantling the structure are not appropriate because of interference with its operation. Assessing the structural condition without removing the individual structural components is known as *non-destructive evaluation* (NDE) or *non-destructive inspection* (NDI).

Many methods have been developed for NDE, and an overview of the various techniques is presented by Witherell.[1] Some techniques are based on visual observations of cracks, such as visual inspection and dye-penetrant inspection. Some are based on the electromagnetic properties of the material, such as magnetic particle inspection and eddy-current inspection. Still other techniques are based on the interpretation of the structural condition by observing the change in the mechanical properties of the structure. The use of vibration test data to determine structural characteristics falls into this last category.

The use of vibration (or modal) testing is an attractive method for determining the global mechanical characteristics of a structure, because techniques for modal data reduction and analysis are well developed for other applications. Existing facilities and methods can be utilized for NDE, and modern data acquisition systems allow the acquisition, processing, storage and analysis of hundreds of channels of data. Since it is desirable to assess the condition of a structure *in situ*, or in its operating environment, the ability to make modal measurements remotely and quickly minimizes the impact on the operation of the structure.

Modal techniques for NDE are typically implemented using finite element model (FEM) update. FEM update methods are based on modifying the FEM stiffness, mass, and/or damping matrices to minimize some measure of error, which is typically a function of the FEM matrices and the measured modal parameters. A review and detailed discussion of the overall field of FEM update are presented by Hemez.[2] Using FEM update-based techniques for NDE can be considered a special case of the general update problem since there are special considerations that are applicable to model refinement in general, but not to NDE specifically. For example, when using FEM update for model refinement, it may be desirable to constrain the material properties of several different elements to be the same

and then update this common parameter. However, for NDE, it is desirable to let these properties vary independently, since the changes are to reflect isolated incidents of damage and not overall errors in modeling assumptions.This makes FEM updating for NDE more difficult than FEM updating for other applications.

The three basic classes of methods for FEM update that are used for NDE are *optimal matrix update*, (see Smith,[3] Zimmerman and Kaouk[4-6]), *sensitivity-based matrix update* (see Hemez and Farhat,[2,7,8] Doebling, et al.,[9] Ricles and Kosmatka[10]), and *eigenstructure assignment* (see Zimmerman and Kaouk,[11] Lim and Kashangaki[12,13,14]). All of these FEM update techniques require that the user select a subset of the measured modes to be correlated with the corresponding modes of the FEM. Normally, the first few modes of the structure are used in the FEM correlation, since they are generally the best identified modes. However, in some situations the higher frequency modes are critical to the location of structural damage, so it is necessary to include them in the set of modes for FEM correlation. Many modes that are below these in frequency do not undergo significant modification as a result of the damage, so they contribute to the computational burden without contributing significantly to the location of the damage. The number of modes is limited not only by the computational burden, but also by the inherent ill-conditioning and statistical bias associated with large-order update problems, as addressed by Cogan, et al.[15] and Hemez and Farhat.[16] Because of this limit, it is important to have a systematic criteria for selecting which modes are most indicative of the structural damage.

Mode selection has been studied previously by Kashangaki,[17] Lim,[18] and Lim.[19] In Ref. [17], Kashangaki presents the modal sensitivity parameter, which is the sensitivity of the FEM eigensolution to changes in each of the elemental stiffness parameters. This pa-

rameter is then used as a pre-test analysis tool for determining which modes should be targeted in the test. In Ref. [18], Lim presents a method of mode selection based on modal cost, which is a measure of the level of energy required to excite a certain mode.

Previous studies (see Kashangaki, et al.,[20] Chen and Garba[21]) have indicated the importance of strain energy in the identification of structural behavior and location of structural damage. This importance can be described in terms of the structural load paths. When a particular vibration mode stores a large amount of strain energy in a particular structural load path, the frequency and displacement shape of that mode are highly sensitive to changes in the impedance of that load path. Thus, strain energy is a logical choice of criteria in model update mode selection. In the case of structures with dominant global behavior, such as a cantilevered beam, the lowest frequency modes may also contain the best overall distributions of structural strain energy. However, for structures that are dominated by local behavior, such as a free truss with distributed mass, the strain energy distribution is not as concentrated in the lowest frequencies. In many cases, the modes that contain vital information about the damage occur at higher frequency, as discussed in Ref. [20].

In this paper, three strategies for mode selection are presented and evaluated. Each strategy selects the damaged modes used to update the FEM of a suspended truss structure. The results will show that it is better to choose those modes that store the highest level of total structural strain energy over the entire structure, and specifically those modes that store the highest level of strain energy in the damaged, rather than the undamaged, structural configuration. The method presented here has a major advantage over previous strain energy-based mode selection techniques: It uses only measured quantities in the criteria function, and thus has lower computational cost than methods that require analytical sensi-

tivity derivatives, such as the method of Ref. [17]. This distinction makes this method suitable for applications that require quick turn-around, such as on-line health monitoring of operational structures.

The remainder of this paper is organized as follows: The first section describes the three mode selection strategies that are to be compared. The second section describes the FEM updating procedure. The third section presents a description of the experimental testbed and procedure. The final section contains the analysis of the model update results and a comparison of the three mode selection strategies.

Mode Selection Strategies

The three mode selection strategies (MSS) examined in this research are:

- MSS 1: Selection of modes based on lowest modal frequency
- MSS 2: Selection of modes in damaged configuration that correspond to the modes that store the highest level of strain energy in the undamaged structural configuration
- MSS 3: Selection of modes that store the highest level of strain energy in the damaged structural configuration

If the measured modes are mass-normalized, the stiffness matrices $[K^u]$ and $[K^d]$ can be estimated using the Moore-Penrose pseudoinverse of the measured flexibility matrix for each modal set.

$$\begin{aligned} [K^u] &= ([\Phi^u][\Lambda^u]^{-1}[\Phi^u]^T)^+ \\ [K^d] &= ([\Phi^d][\Lambda^d]^{-1}[\Phi^d]^T)^+ \end{aligned} \tag{1}$$

This formulation of the stiffness matrix is equivalent to a static reduction with respect to the measured degrees of freedom in the limit that all significant structural modes are mea-

sured, as described in Ref. [22] and Ref. [23]. Since the number of measured modes is typically smaller than the number of measurement degrees of freedom, these matrices are in general reduced-rank.

The general expression for the strain energy stored in a structure with global stiffness matrix $[K]$ when subjected to global displacement set $\{x\}$ is

$$U = \frac{1}{2}\{x\}^T[K]\{x\} \tag{2}$$

The modal strain energy (i.e. the strain energy stored in mode *j*) can be determined by deflecting the structure according to the modal displacement shape, $\{\phi_j\}$ to get

$$U_j = \frac{1}{2}\{\phi_j\}^T[K]\{\phi_j\} \tag{3}$$

for each measured mode j in the identified modal set. For mass-normalized modes, when the full stiffness matrix is known exactly, Eq. (3) yields the modal eigenvalues. Substituting the undamaged mode shapes $[\Phi^u]$ and stiffness matrix $[K^u]$ into Eq. (3), the strain energy computation for MSS 2 can be written

$$U_j = \frac{1}{2}\{\phi_j{}^u\}^T([\Phi^u][\Lambda^u]^{-1}[\Phi^u]^T)^+\{\phi_j^u\} \tag{4}$$

Similarly, the strain energy computation for MSS 3 can be written

$$U_j = \frac{1}{2}\{\phi_j{}^d\}^T([\Phi^d][\Lambda^d]^{-1}[\Phi^d]^T)^+\{\phi_j^d\} \tag{5}$$

It should be noted that the stiffness matrix $[K]$ of Eq. (3) can be computed using either the identified modal set, as in Eq. (1), or a condensation from a larger dimension FEM stiffness matrix. If a condensed FEM matrix were used in the energy computation, however, it would not be possible to use MSS 3 to select modes for the update. This occurs because MSS 3 depends upon the stiffness matrix of the damaged structure, which is unknown prior to the

model update. Thus, the experimentally determined stiffness matrix of Eq. (1) is used so that MSS 3 can be properly implemented.

It should also be noted that the expressions of strain energy in Eq. (4) and Eq. (5) are actually degenerate cases of the full strain energy expression in Eq. (3) because the measured stiffness matrix is incomplete and because the measured mode shapes are not perfectly measured nor perfectly mass-normalized. Thus, the expressions in Eq. (4) and Eq. (5) are not actually strain energy, but are approximations of the modal strain energy content based solely on the measured modal parameters.

When using FEM update to locate damage, the damage state of the structure is determined by updating the model to match the modes of the damaged structure. Therefore, the modes used in the update must be selected from the damaged modal set. MSS 1 and MSS 3 use the damaged modes directly as criteria, so the selection process is straightforward. However, MSS 2 uses the strain energy of the undamaged modes as criteria. The modes used in the update under MSS 2 are actually the damaged modes that correspond to the selected undamaged modes. To select these corresponding modes, an equivalence must be determined between the modes of the undamaged structure and the modes of the damaged structure. This can be accomplished by comparing the Modal Assurance Criterion (MAC) between the two modal sets. The MAC between two modal vectors $\{\Phi_i\}$ and $\{\Phi_j\}$ is defined in Ref. [24] as

$$\mathrm{MAC}_{i,j} = \frac{(\{\Phi_i\}^T\{\Phi_j\})^2}{(\{\Phi_i\}^T\{\Phi_i\})(\{\Phi_j\}^T\{\Phi_j\})} \tag{6}$$

and is usually expressed as a percentage. For each undamaged mode selected using MSS 2, a corresponding damaged mode is selected that produces the highest MAC with that un-

damaged mode. It can sometimes be difficult to locate a damaged mode that produces a high MAC with a particular undamaged mode, especially when the damage causes large changes in the mode shapes between the undamaged and damaged structural configurations. In this case, strategies such as MSS 1 or MSS 3 that do not require the definition of such an equivalence are advantageous. It should also be noted that the modes which are the most sensitive to the damage, and therefore undergo the largest change as a result of the damage, may have a very low MAC with the corresponding modes in the undamaged modal set. Therefore, MAC is generally not a very good criteria for mode selection for model update-based damage detection, but is useful for determining equivalency between sets of modes.

Finite Element Model Update Procedure

The FEM update will be accomplished in this study using the Sensitivity Based Element By Element (SB-EBE) algorithm.[2,7,8] This algorithm iteratively adjusts the physical parameters of the FEM on an element-by-element basis until the out-of-balance forces in the model are minimized, producing the best agreement between a chosen set of measured modal parameters and the FEM. The accuracy of the damage detection results in an experiment with a known level of damage can be assessed by comparing the change in member cross-sectional area produced by the model update to the actual change expected based on the known damage configuration. The level of ambiguity, or uniqueness, of the damage detection result can be determined qualitatively by examining the changes in cross-sectional area of each member. In some cases, one update result may be more accurate in terms of total error in member cross-sectional areas, but another update may be more accurate if it has a more unique indication of the damage location. In this paper, the average percent error

in cross-sectional areas over all structural elements

$$E = \left(\frac{1}{N_e}\right) \sum_{e = 1 \ldots N_e} \left| \frac{(\hat{A}^{(e)} - A^{(e)})}{A^{(e)}} \right| \times 100\% \tag{7}$$

is used as the measure of damage detection accuracy. It should be noted that any elemental parameter, not just cross-sectional area, could be varied in the update procedure. Cross-sectional area was chosen so that the mass and stiffness could be updated simultaneously, which is consistent with the damage case being studied in this research (i.e. total removal of a member).

The updating for each damage case in this research was performed on an IBM RISC 6000/550 computer. The update results shown required 2 or 3 updating iterations. The CPU time was about 200 seconds per iteration and the memory requirement was about 25 million words (at 64 bytes per word). It should be noted that the large memory requirement results from a suboptimal numerical implementation, and not from the SB-EBE updating formulation itself.

Experimental Testbed and Procedure

The experimental testbed used for this study is a scale model precision truss known as the Model Update / Damage Detection Experiment (MUDDE) truss, shown in Figure 1. It consists of 8 bays, each 1/2 meter in length. The structure has 8 lumped masses connected to it as shown in Figure 2. The 3 larger masses weigh 5 lbs. each, and the 5 smaller masses weigh 1 lb. each, so that the non-structural mass is about 50% of the total mass. Preliminary testing and finite element modeling indicated that the structure's lowest modes are dominated by rotation of the large masses, causing the strain energy in those modes to be con-

centrated around those masses. This localized modal behavior makes the MUDDE truss an appropriate representation of large spacecraft structures such as International Space Station Alpha.

To experimentally simulate the effect of damage, the following procedure was followed. First, a modal survey of the nominal structure was conducted to obtain a set of undamaged modes. Next, a member on the structure was removed, and the modal survey was repeated. This member was replaced and the procedure was repeated, for a total of 3 damage cases. The nominal survey was repeated after the final damage case, to measure any changes that may have occurred in the structure. Damage Case 1 was a longeron adjacent to one of the 5 lb. masses. Damage Case 2 was a longeron located near the center of the truss, and Damage Case 3 was a diagonal member on the upper surface of the truss. The members used in the damage cases are noted in Figure 2.

The first five measured modes were used to correlate the undamaged finite element model. To locate the damage, the modes measured by testing the structure in each damage configuration were used in the update algorithm. The three mode selection strategies were used to determine three sets of modes to use in the update for each damage case. The results of these updates provide the basis for comparing the relative merit of the mode selection strategies.

The structure was instrumented using piezoelectric accelerometers mounted in triaxial blocks on each node ball of the structure. Since there were 111 DOF measured (36 nodes, each with 3DOF, plus 3 driving points) and only 57 channels available, the data for each damage case was collected in two experiments. The offsets of the sensors from the center

of each node ball were measured and incorporated into the finite element model.

Force inputs were applied at 3 locations. These input locations were chosen in an attempt to excite as many measurable modes as possible. The excitations were made by a modal shaker via a stinger to ensure that forces applied to the structure were effectively uniaxial. The force level was measured by a piezoelectric load cell, which was located between the stinger and the structure. Additionally, a driving point accelerometer was placed in line with the load cell at each input location, to obtain a collocated force-acceleration measurement. These driving point measurements were necessary in order to properly mass-normalize the mode shapes.

The extraction of normal modal parameters from the modal survey data consisted of three phases: Time-domain identification of a state-space model, frequency-domain fit of the mode shapes including residual flexibility terms, and a normalization procedure to ensure that the modal parameters are properly mass-normalized. The complete identification procedure is discussed in detail by Peterson and Alvin.[25] A sample FRF reconstruction is shown in Figure 3 to demonstrate the accuracy of the modal curve fit. The clusters of modes around 80 Hz are the first bending modes of the truss diagonals, and the clusters of modes around 140 Hz are the first bending modes of the truss longerons and battens.

Analysis of Model Update Results

As mentioned previously, implementation of MSS 2 requires the definition of an equivalency between the measured modes of the undamaged structure and those of each damage structural configuration. The identified modes from each damage case were correlated with the undamaged modal set, and the results are shown in Table 1, Table 2, and Table 3. The

Table 1. Correlation of Modes for Damage Case 1

Undamaged Structure (Modes in Order of Decreasing Modal Strain Energy)		Damaged Structure (Modes that Correspond with Highest MAC to Undamaged Modes)		MAC between Damaged and Undamaged Modes (%)
Mode	**Freq. (Hz)**	**Mode**	**Freq. (Hz)**	
1	46.82	2	46.86	69.86
34	85.53	37	85.49	96.32
3	48.59	6	61.45	50.83
6	54.34	4	52.99	86.70
45	92.49	(a)		
83	167.84	97	167.55	62.80
7	62.93	(a)		
51	96.96	53	96.64	63.53
54	101.73	56	101.53	92.14
33	84.91	36	84.87	95.77

a. No mode with adequate correlation found

Table 2. Correlation of Modes for Damage Case 2

Undamaged Structure (Modes in Order of Decreasing Modal Strain Energy)		Damaged Structure (Modes that Correspond with Highest MAC to Undamaged Modes)		MAC between Damaged and Undamaged Modes (%)
Mode	**Freq. (Hz)**	**Mode**	**Freq. (Hz)**	
1	46.82	(a)		
34	85.53	34	84.20	46.77
3	48.59	(a)		
6	54.34	9	54.19	44.04
45	92.49	53	101.74	36.58
83	167.84	99	167.76	67.44
7	62.93	10	63.90	38.23
51	96.96	50	96.86	95.76
54	101.73	(a)		
33	84.91	34	84.20	80.91

a. No mode with adequate correlation found

Table 3. Correlation of Modes for Damage Case 3

Undamaged Structure (Modes in Order of Decreasing Modal Strain Energy)		Damaged Structure (Modes that Correspond with Highest MAC to Undamaged Modes)		MAC between Damaged and Undamaged Modes (%)
Mode	**Freq. (Hz)**	**Mode**	**Freq. (Hz)**	
1	46.82	2	46.97	83.01
34	85.53	39	85.10	62.65
3	48.59	3	48.29	41.72
6	54.34	6	54.24	97.41
45	92.49	49	92.43	47.33
83	167.84	97	167.42	64.83
7	62.93	(a)		
51	96.96	51	97.19	76.11
54	101.73	53	98.12	63.51
33	84.91	(a)		

a. No mode with adequate correlation found

modes of the undamaged structure are listed in order of decreasing modal strain energy. The correlations were determined by comparing the MAC values between the two modal sets. Pairs of modes that demonstrated high MAC values are listed on the same row in the tables. In some cases no significant MAC values could be found, so no adequate correlation could be defined. It should be noted that even in the case of low MAC, the modes were still identified well according to other modal quality indicators (see Ref. [25]), and are therefore known to be representative of the actual structural dynamics and are not mathematical artifacts of the identification algorithm.

The sets of modes selected using each strategy are shown in Table 4. MSS 1 uses the lowest frequency modes for each damage case. MSS 2 uses the modes in each damage case that correspond to the modes of the undamaged case that have the maximum modal strain

Table 4. Modal Sets Selected by Each Mode Selection Strategy

Mode Selection Strategy	Description of Strategy	Modes Selected for Damage Case 1	Modes Selected for Damage Case 2	Modes Selected for Damage Case 3
MSS 1	Modes with Lowest Frequency in Each Damage Case	1, 2, 3, 4, 5	1, 2, 3, 4, 5	1, 2, 3, 4, 5
MSS 2 [(a)]	Modes in Each Damage Case Corresponding to Undamaged Modes with Highest Strain Energy	2, 37, 4, 56, 36	34, 9, 99, 10, 50	2, 6, 97, 51, 53
MSS 3 [(a)]	Modes with Highest Strain Energy in Each Damage Case	1, 4, 9, 25, 50	1, 100, 99, 47, 71	1, 83, 88, 105, 106

a. Modes listed in order of decreasing modal strain energy level

energy. For the actual implementation of MSS 2, the MAC values were used as an additional criteria to ensure that poorly correlated modes were not used in the update. Because the mode shapes change for each damage case, the undamaged modes with maximum modal strain energy did not always correspond to the same damaged modes. MSS 3 uses the modes in each damage case that have the maximum modal strain energy for that damage case. The modes in Table 4 for MSS 2 and MSS 3 are listed in order of decreasing modal strain energy.

To assess the relative accuracy of the model updates, the average errors in member cross-sectional areas, shown in Table 5, are compared. In all three damage cases, MSS 2

Table 5. Average Member Cross-Sectional Area Error (in Percent)

Mode Selection Strategy	Damage Case 1	Damage Case 2	Damage Case 3
MSS 1	0.7204	6.355	4.297
MSS 2	0.08908	2.681	2.870

Table 5. Average Member Cross-Sectional Area Error (in Percent)

Mode Selection Strategy	Damage Case 1	Damage Case 2	Damage Case 3
MSS 3	0.08431	0.6131	2.126

shows an improvement in update result over MSS 1. Similarly, MSS 3 shows an improvement compared to MSS 2. These consistent results support the hypothesis that the strategy of selecting modes based on strain energy content is generally better than selecting modes based on lowest modal frequency. Additionally, the results also support the conclusion that selecting the modes based on the strain energy distribution in the damaged structural configuration is better than selecting modes based on the strain energy distribution in the undamaged structure.

The changes in cross-sectional member area resulting from the model updates for Damage Case 1 are shown for the three mode selection strategies in Figure 4, Figure 5, and Figure 6. In each of these figures, the dashed line denotes the actual location of the damage. The change in each member area is determined by averaging the changes in the cross-sectional area of the five Bernoulli-Euler beam elements that compose the member. The large change at one truss member in each of these figures indicates that the damage is located using each of these modal set selection strategies. However, a more accurate assessment of the damage location is achieved using MSS 2 and MSS 3. The changes in cross-sectional member area resulting from the model updates for Damage Case 2 are shown for the three mode selection strategies in Figure 7, Figure 8, and Figure 9. Examination of these updates indicates that the damage is not identified by MSS 1, and that it is identified better with MSS 3 than with MSS 2. The changes in cross-sectional member area resulting from the

model updates for Damage Case 3 are shown for the three mode selection strategies in Figure 10, Figure 11, and Figure 12. These plots indicate that the damage is not conclusively located for any of these updates, but the error in the update results once again gets progressively smaller from MSS 1 to MSS 2, and from MSS 2 to MSS 3. Also, for MSS 2 and MSS 3, the update changes are more localized to the damaged region of the structure than for MSS 1.

By comparing the update results of Figure 4 through Figure 12, and taking into account the members removed in each damage case, the effect of the local nature of the structural change can be seen. For example, in Damage Case 1, when a longeron adjacent to one of the large structural masses is removed, the effect on the dynamic behavior of the structure is both significant and localized, leading to a damage case that is identified well by the update algorithm. In Damage Case 2, when a longeron away from the large masses is removed, a smaller, still localized change in the dynamic character of the structure is produced, leading to a damage identification that is more ambiguous than that of Damage Case 1. In Damage Case 3, when a diagonal member is removed, the major load paths of the structure are not significantly affected, and thus the changes in the dynamic behavior of the structure are not localized to a particular region of the structure, making identification of the structural damage difficult.

Conclusion

A series of strategies for selecting the subset of identified modes that are used in a finite element model correlation procedure have been compared. The results indicate that using the maximum modal strain energy over the entire structure as a criteria provides more ac-

curate update results than using the minimum modal frequency. The fundamental significance of using modal strain energy as an indicator of the relative importance of modes can be seen by examining the form of the strain energy equation. The modes that yield the highest value of strain energy are the modes that tend to "stretch" the stiffness matrix the most. These modes will have the most significant contribution to the stiffness matrix itself, and thus provide the best information about changes to the elemental stiffness parameters of the structure. As demonstrated, the modes with highest overall strain energy are not necessarily the lowest frequency modes, and thus may not be selected for use in the model update under conventional modal frequency-based selection criteria.

The results also indicate that using the modes that have maximum strain energy in the damaged structural configuration is better than using the modes that have maximum strain energy in the undamaged configuration for two reasons: First, the modes selected using a model of the damaged structure provide more accurate update results, since they provide more information about the changes in the structural load paths resulting from damage. Second, using the modes from the damaged configuration eliminates the need to find a one-to-one correspondence between the undamaged and damaged modes. This implies that criteria based on the nominal structural configuration will in general be inferior to criteria based on the damaged structural configuration. However, to use the damaged structural configuration in the selection strategy prior to performing the update requires the formulation of an experimentally-based model. Such a model requires accurate identification and mass-normalization of the damaged structure's mode shapes, which can be difficult when the response of the structure is modally dense. The method presented in this paper provides a computationally efficient criteria for selecting modes based solely on the modal parame-

ters extracted from the measured data.

Acknowledgments

This research was conducted in the McDonnell-Douglas Aerospace Structural Dynamics and Control Laboratory at the University of Colorado at Boulder. Support was provided by NASA Grant NAGW-1388 through the Center for Space Construction. It was also supported in part by a donation from the Shimizu Corporation and a donation from the McDonnell Douglas Foundation. The first author was supported by a National Science Foundation Graduate Fellowship and by Los Alamos National Laboratory Directed Research and Development Project #95002.

References

[1]Witherell, C.E., *Mechanical Failure Avoidance: Strategies and Techniques*, McGraw-Hill, New York, 1994.

[2]Hemez, F.M., "Theoretical and Experimental Correlation between Finite Element Models and Modal Tests in the Context of Large Flexible Space Structures," Ph. D. Dissertation, Dept. of Aerospace Engineering Sciences, Univ. of Colorado, Rept. CU-CAS-93-18, Boulder, CO, August 1993.

[3]Smith, S.W., "Application Strategies for Structure Identification with Optimal-Matrix Updates," *Proceedings of the 11th International Modal Analysis Conference*, Orlando, FL, February 1993.

[4]Zimmerman, D.C. and Kaouk, M., "Structural Damage Detection Using a Subspace Rotation Algorithm," AIAA-92-2521-CP, *Proceedings of the 33rd AIAA/ASME/ASCE/AHS/ASC Structures, Structural Dynamics, and Materials Conference*, Dallas, TX, April 1992.

[5]Kaouk, M. and Zimmerman, D.C., "Structural Damage Assessment Using a Gen-

eralized Minimum Rank Perturbation Theory," AIAA-93-1483-CP, *Proceedings of the 34th AIAA/ASME/ASCE/AHS/ASC Structures, Structural Dynamics, and Materials Conference*, La Jolla, CA, April 1993.

[6]Kaouk, M. and Zimmerman, D.C., "Evaluation of the Minimum Rank Update in Damage Detection: An Experimental Study," *Proceedings of the 11th International Modal Analysis Conference*, Orlando, FL, February 1993.

[7]Hemez, F. M. and Farhat, C., "Locating and Identifying Structural Damage Using a Sensitivity-Based Model Updating Methodology," *Proceedings of the 34th AIAA/ASME/ASCE/AHS/ASC Structures, Structural Dynamics, and Materials Conference*, La Jolla, CA, April 1993, pp. 2641-2653.

[8]Farhat, C. and Hemez, F. M., "Updating Finite Element Dynamic Models Using an Element-By-Element Sensitivity Methodology," *AIAA Journal*, Vol. 31, No. 9, September 1993, pp. 1702-1711.

[9]Doebling, S.W., Hemez, F.M., Barlow, M.S., Peterson, L.D., and Farhat, C., "Damage Detection in a Suspended Scale Model Truss via Modal Update," *Proceedings of the 11th International Modal Analysis Conference*, Orlando, FL, February 1993.

[10]Ricles, J.M. and J.B. Kosmatka, "Damage Detection in Elastic Structures Using Vibratory Residual Forces and Weighted Sensitivity," *AIAA Journal*, Vol. 30, No. 9, 1992, pp. 2310–2316.

[11]Zimmerman, D.C. and Kaouk, M., "Eigenstructure Assignment Approach for Structural Damage Detection," *AIAA Journal*, Vol. 30, No. 7, July 1992.

[12]Lim, T.W., "Structural Damage Detection Using Constrained Eigenstructure Assignment," *Journal of Guidance Control and Dynamics*, Vol. 18, No. 3, 1995, pp. 411–418.

[13]Lim, T.W. and Kashangaki, T. A-L., "Structural Damage Detection of Space Truss Structures Using Best Achievable Eigenvectors," *AIAA Journal*, Vol. 32, No. 5, May 1994, pp. 1049-1057.

[14]Kashangaki, T. A.-L., *Damage Location and Model Refinement for Large Flexi-*

ble Space Structures Using a Sensitivity Based Eigenstructure Assignment Method, Ph. D. Dissertation, University of Michigan, Ann Arbor, MI, 1992.

[15]Cogan, S., Lallement, G., Ayer, F., and Ben-Haim, Y. "Updating Linear Elastic Models with Modal Selective Sensitivity," *Inverse Problems in Engineering*, Vol. 2, 1995, pp. 29-47.

[16]Hemez, F. M., and Farhat, C., "Bypassing the Numerical Difficulties Associated with the Updating of Finite Element Matrices," *AIAA Journal*, Vol. 33, No. 3, March 1995, pp. 539--546.

[17]Kashangaki, T. A.-L., "Mode Selection for Damage Detection using the Modal Sensitivity Parameter," AIAA Paper No. 95-1342-CP, *Proceedings of the 36th AIAA/ ASME/ASCE/AHS/ASC Structures, Structural Dynamics, and Materials Conference*, New Orleans, LA, April 1995, pp. 1535-1542.

[18]Lim, T. W., "Sensor Placement for On-Orbit Modal Testing," AIAA Paper No. 91-1184-CP, *Proceedings of the 32nd AIAA/ASME/ASCE/AHS/ASC Structures, Structural Dynamics, and Materials Conference*, April 1991, pp. 2977-2985.

[19]Lim, K.B., "Method for Optimal Actuator and Sensor Placement for Large Flexible Structures," *Journal of Guidance, Control, and Dynamics*, Vol. 15, No. 1, Jan.-Feb. 1992, pp. 49-57.

[20]Kashangaki, T. A-L., Smith, S.W., and Lim, T.W., "Underlying Modal Data Issues for Detecting Damage in Truss Structures," AIAA Paper No. 92-2264-CP, *Proceedings of the 33rd AIAA/ASME/ASCE/AHS/ASC Structures, Structural Dynamics, and Materials Conference*, April, 1992.

[21]Chen, J.C. and Garba, J.A., "On-Orbit Damage Assessment for Large Space Structures," *AIAA Journal*, Vol. 26, No. 9, Sept. 1988.

[22]Alvin, K.F., "Second Order Structural Identification via State Space-Based System Realizations," Ph. D. Dissertation, Dept. of Aerospace Engineering Sciences, Univ. of Colorado, Boulder, CO, April 1993.

[23]Alvin, K.F., Peterson, L.D. and Park, K.C., "A Method for Determining Minimum-Order Mass and Stiffness Matrices from Modal Test Data," *AIAA Journal*, Vol. 33, No. 1, pp. 128-135, 1995.

[24]Ewins, D.J., *Modal Testing: Theory and Practice*, Wiley, 1984.

[25]Peterson, L.D. and Alvin, K.F., "A Time and Frequency Domain Procedure for Identification of Structural Dynamic Models," *Proc. of 35th AIAA/ASME/ASCE/AHS/ASC Structures, Structural Dynamics, and Materials Conference*, 1994, AIAA Paper No. 94-1731. Submitted to *Journal of Sound and Vibration*.

[26]Juang, J.N. and Pappa, R.S., "An Eigensystem Realization Algorithm for Modal Parameter Identification and Model Reduction," *Journal of Guidance, Control, and Dynamics*, Vol. 8, No. 5, pp 620-627, 1985.

[27]Peterson, L.D., "Efficient Computation of the Eigensystem Realization Algorithm," *Journal of Guidance, Control, and Dynamics*, Vol. 18, No. 3, pp. 395-403, 1995.

[28]Alvin, K.F and Park, K.C., "Second-Order Structural Identification Procedure via State-Space-Based System Identification," *AIAA Journal*, Vol. 32, No. 2, pp. 397-406, 1994.

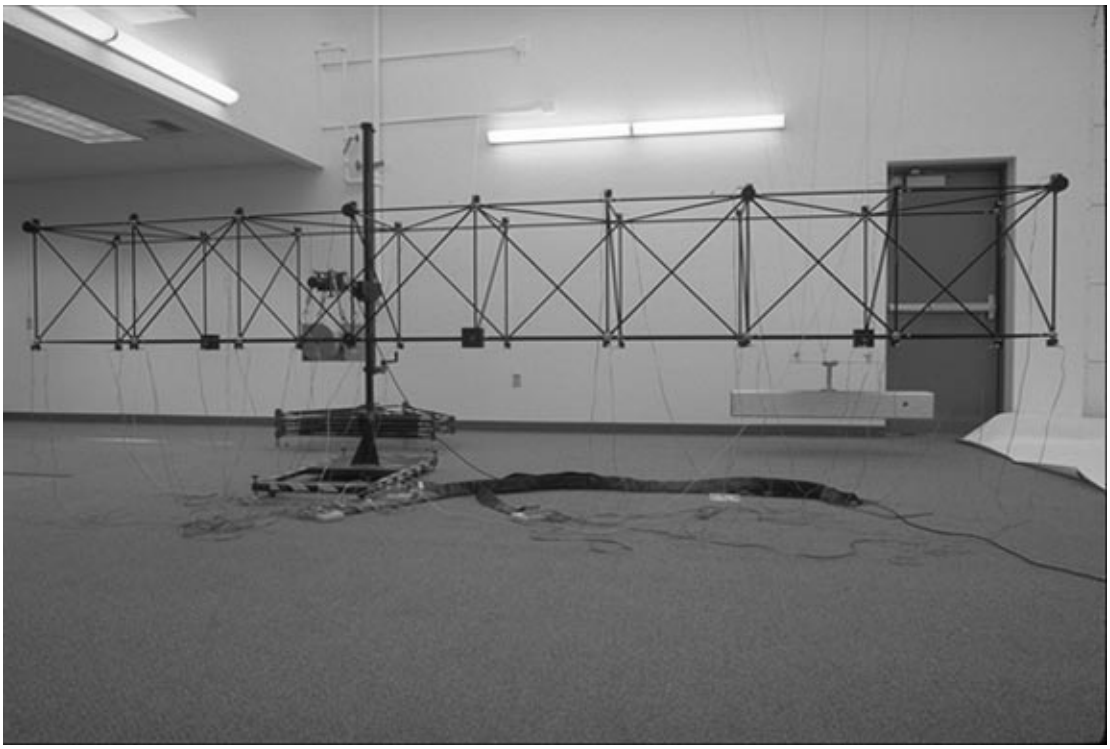

Figure 1: Photo of MUDDE Truss

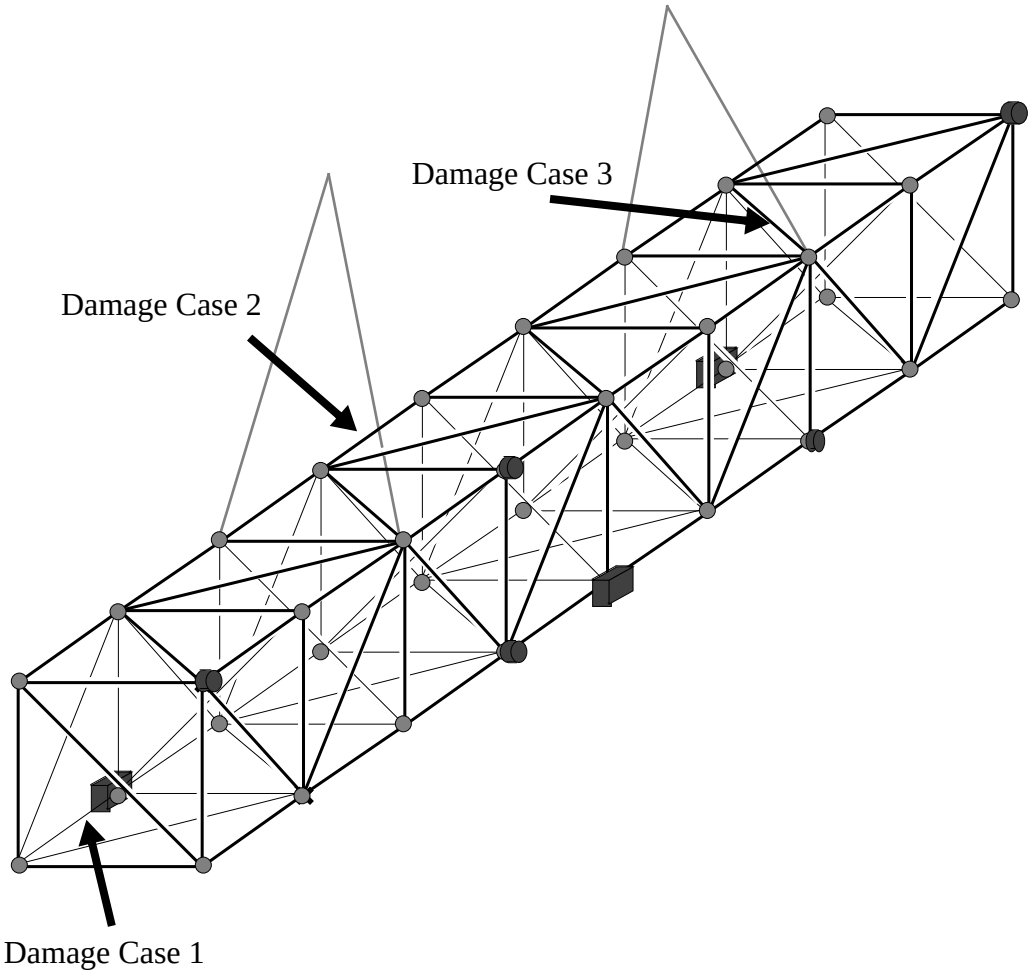

Figure 2: Diagram of Truss Showing Members Used in Damage Cases

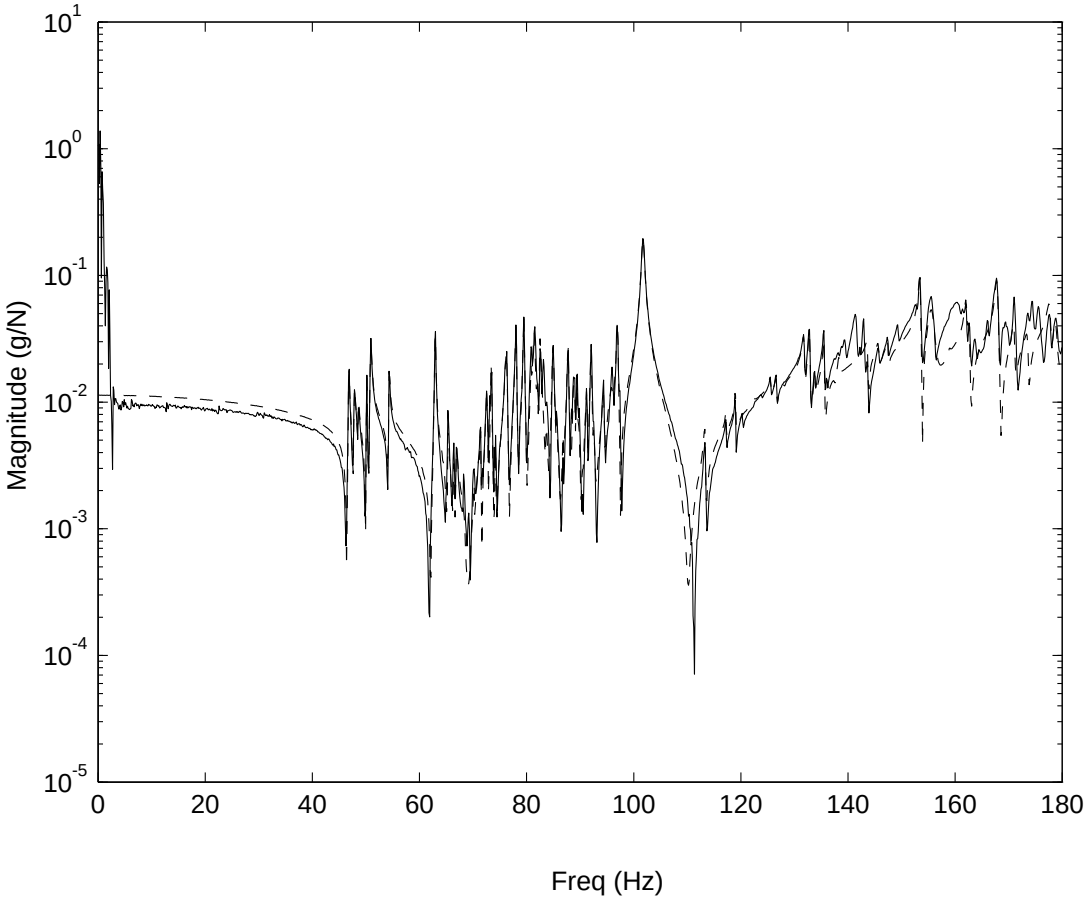

Figure 3: Sample Driving Point FRF and Identified Reconstruction for Undamaged MUDDE Test Structure

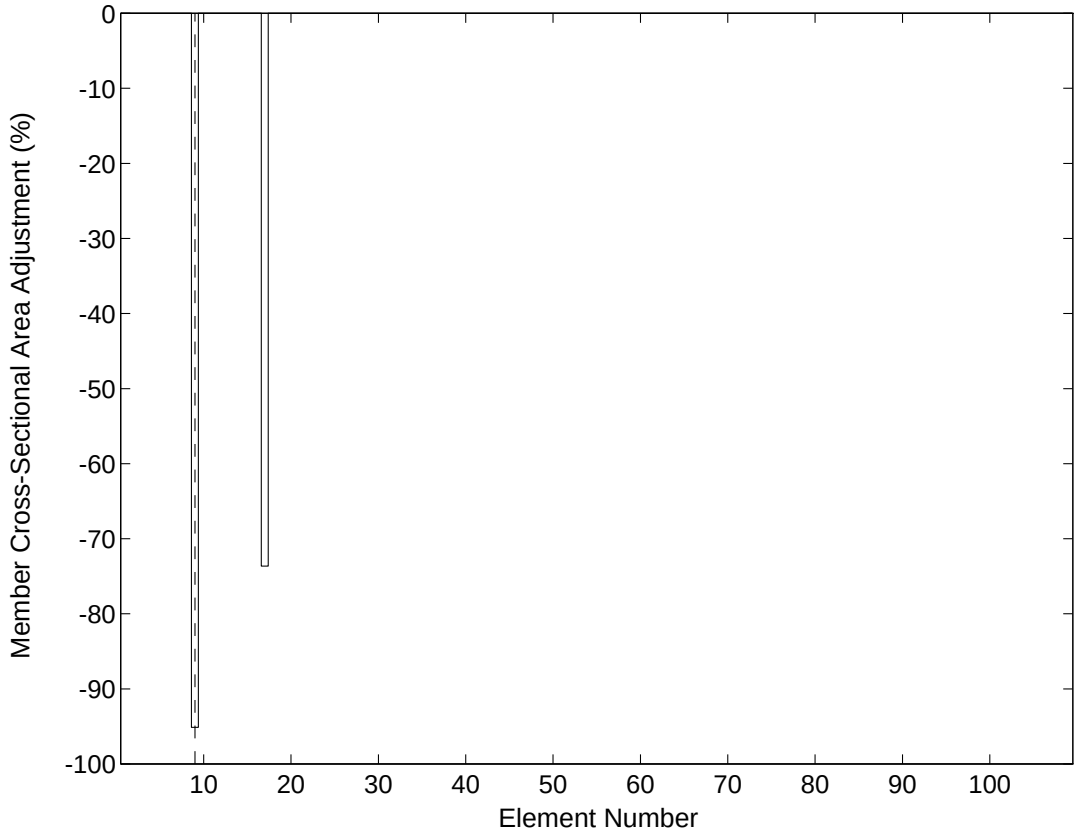

Figure 4: Model Update Results for Damage Case 1, Mode Selection Strategy 1 (Dashed Line Indicates Actual Damaged Member)

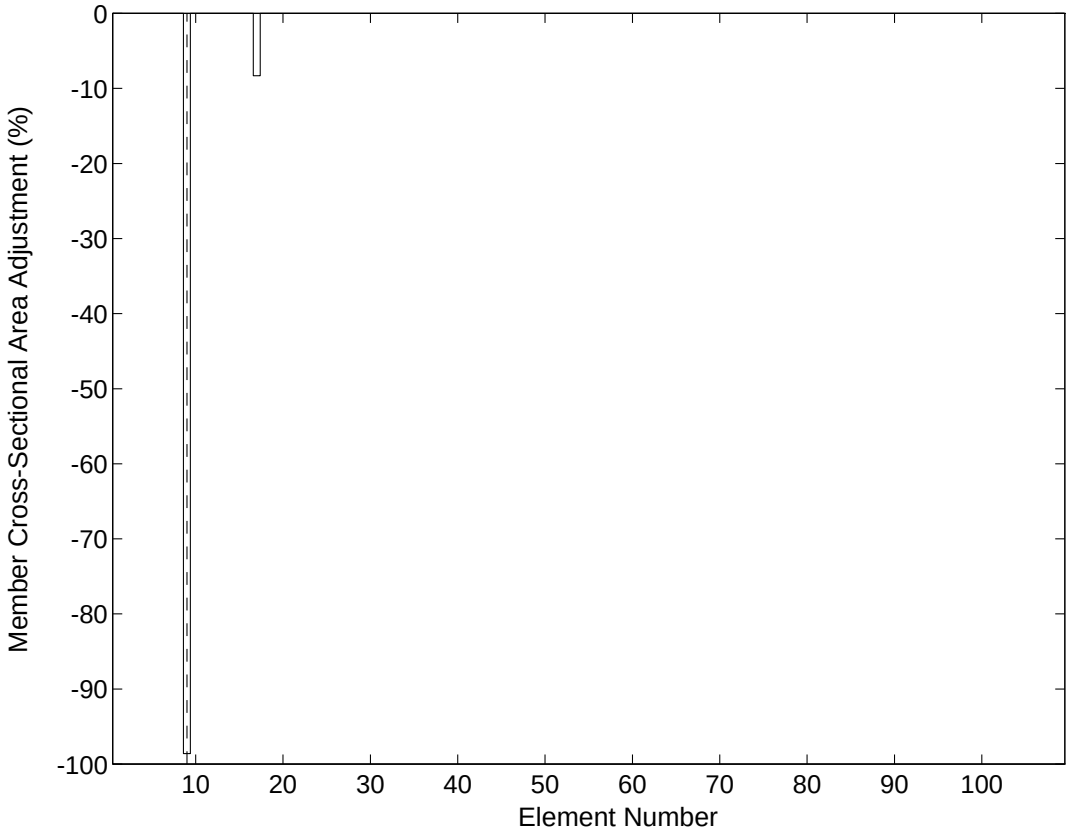

Figure 5: Model Update Results for Damage Case 1, Mode Selection Strategy 2 (Dashed Line Indicates Actual Damaged Member)

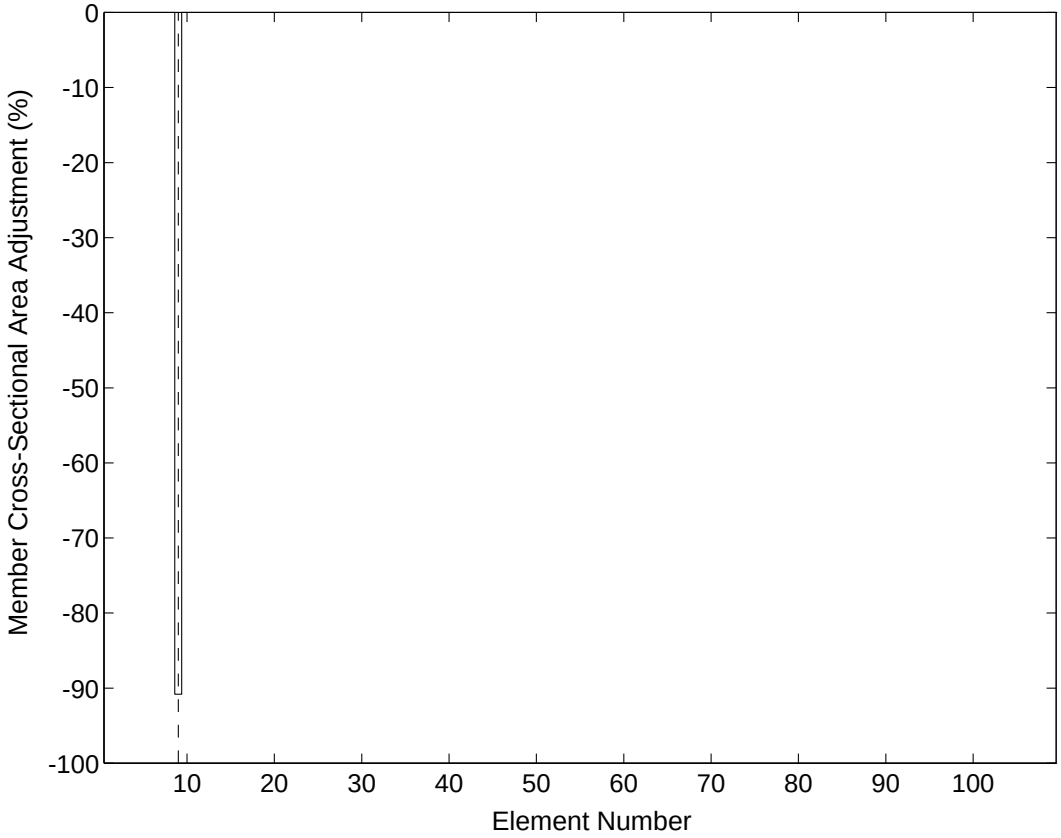

Figure 6: Model Update Results for Damage Case 1, Mode Selection Strategy 3 (Dashed Line Indicates Actual Damaged Member)

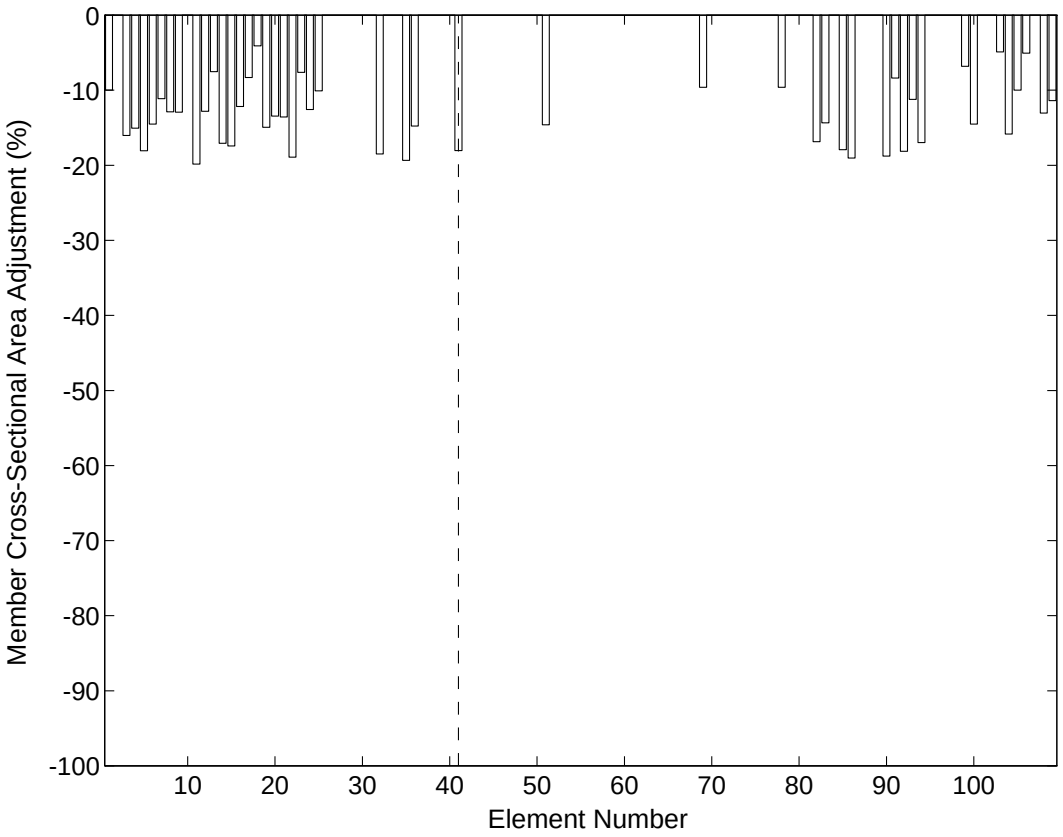

Figure 7: Model Update Results for Damage Case 2, Mode Selection Strategy 1 (Dashed Line Indicates Actual Damaged Member)

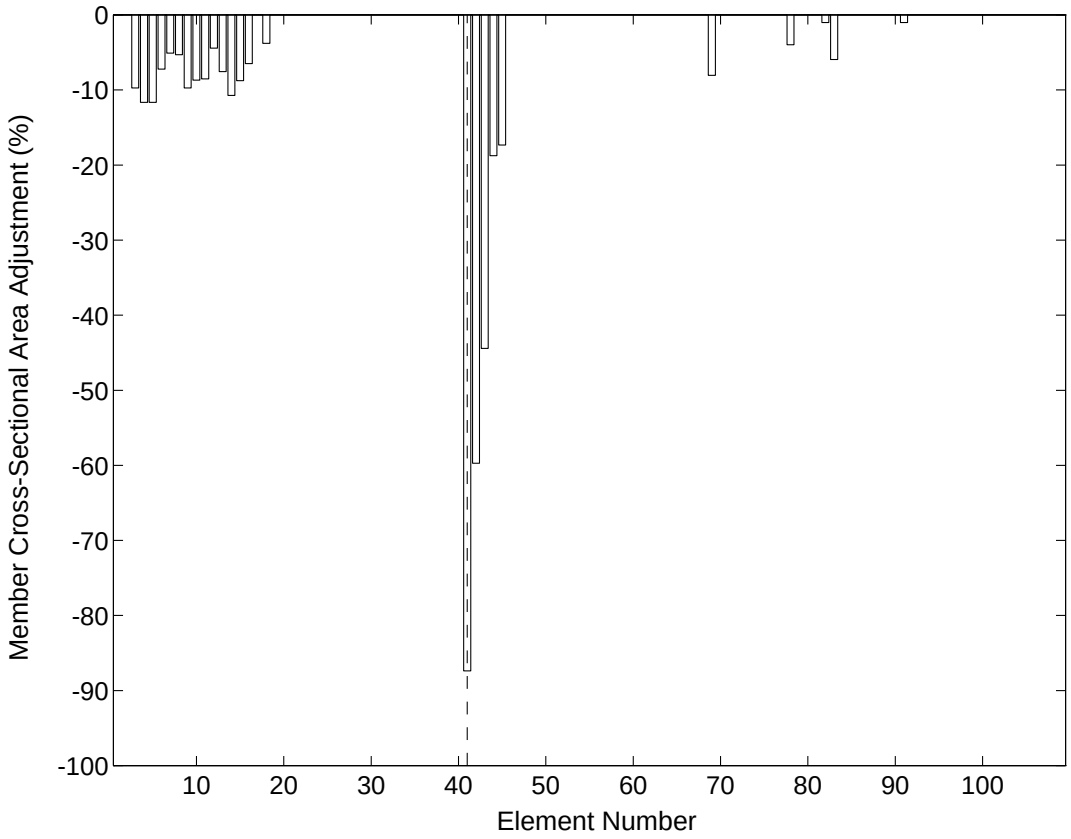

Figure 8: Model Update Results for Damage Case 2, Mode Selection Strategy 2 (Dashed Line Indicates Actual Damaged Member)

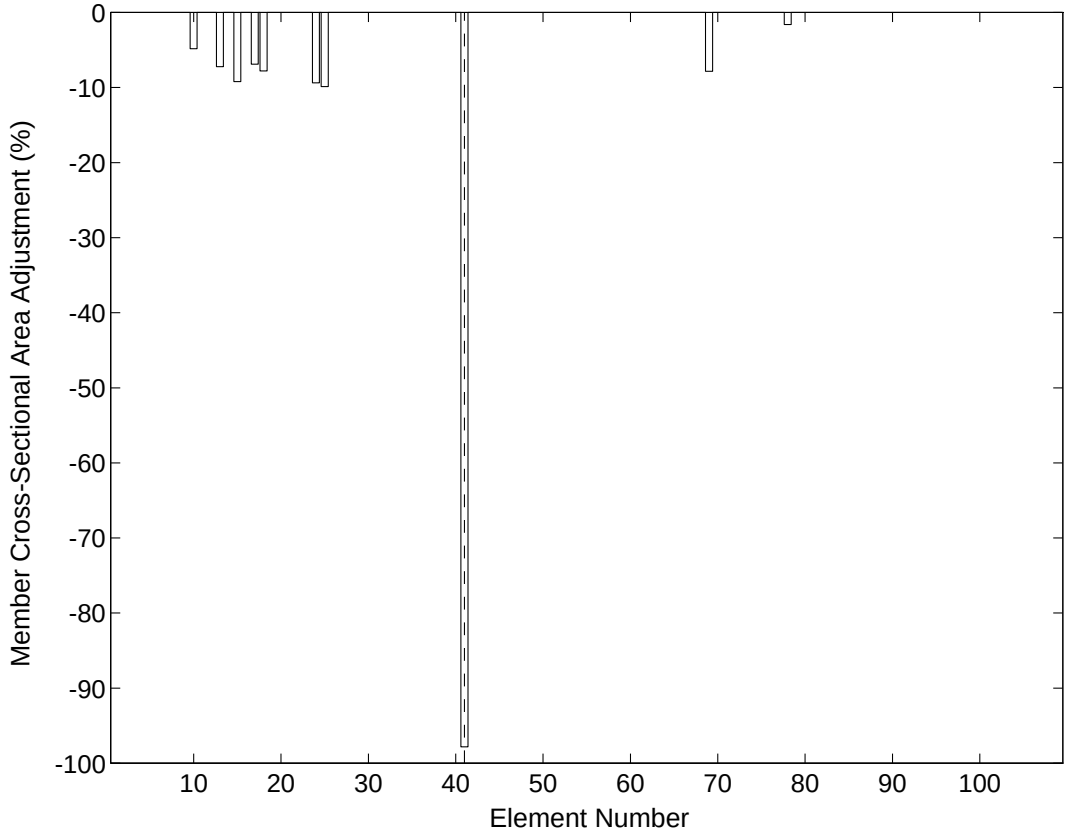

Figure 9: Model Update Results for Damage Case 2, Mode Selection Strategy 3 (Dashed Line Indicates Actual Damaged Member)

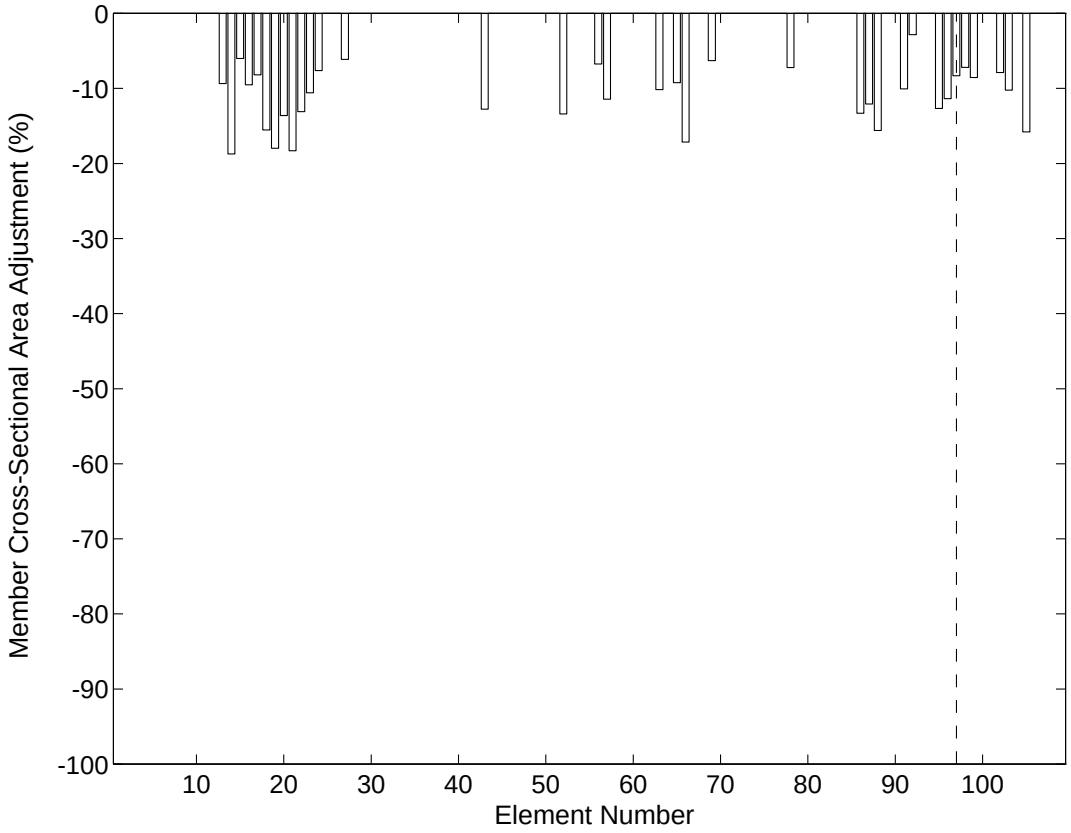

Figure 10: Model Update Results for Damage Case 3, Mode Selection Strategy 1 (Dashed Line Indicates Actual Damaged Member)

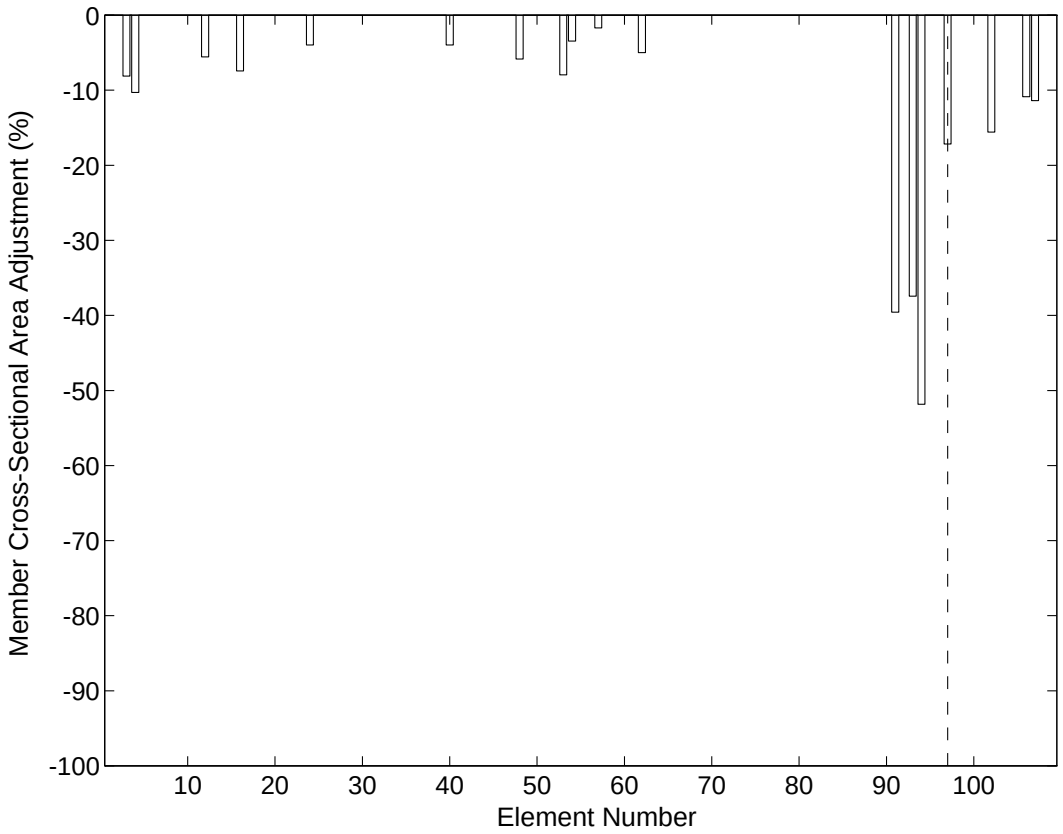

Figure 11: Model Update Results for Damage Case 3, Mode Selection Strategy 2 (Dashed Line Indicates Actual Damaged Member)

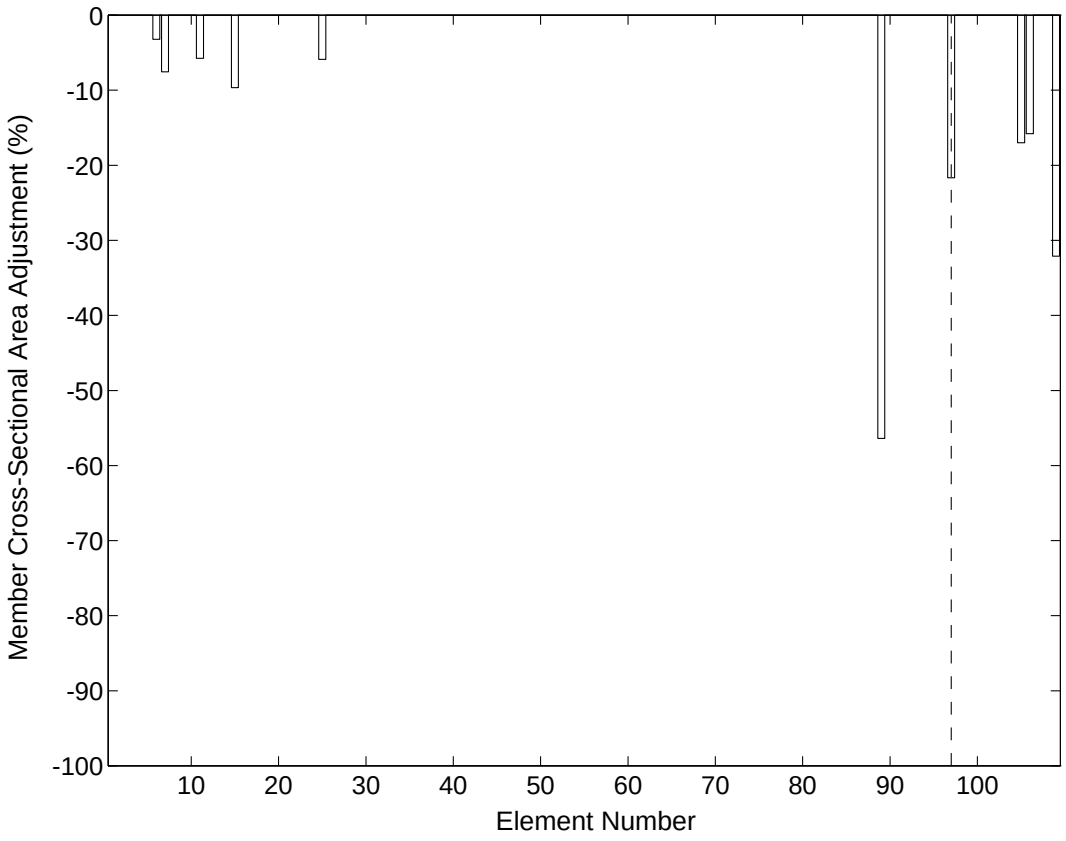

Figure 12: Model Update Results for Damage Case 3, Mode Selection Strategy 3 (Dashed Line Indicates Actual Damaged Member)

List of Figure Captions